

Revealing the non-adiabatic and non-Abelian multiple-band effects via anisotropic valley Hall conduction in bilayer graphene

Ci Li,^{1, 2, *} Matisse Wei-Yuan Tu,^{3, †} and Wang Yao^{1, 2}

¹*Department of Physics, The University of Hong Kong, Hong Kong, China*

²*HKU-UCAS Joint Institute of Theoretical and Computational Physics at Hong Kong, China*

³*Department of Physics, National Sun Yat-sen University, Taiwan*

Many quantum materials of interest, ex., bilayer graphene, possess a number of closely spaced but not fully degenerate bands near the Fermi level, where the coupling to the far detuned remote bands can induce Berry curvatures of the non-Abelian character in this active multiple-band manifold for transport effects. Under finite electric fields, non-adiabatic interband transition processes are expected to play significant roles in the associated Hall conduction. Here through an exemplified study on the valley Hall conduction in AB-stacked bilayer graphene, we show that the contribution arising from non-adiabatic transitions around the bands near the Fermi energy to the Hall current is not only quantitatively about an order-of-magnitude larger than the contribution due to adiabatic inter-manifold transition with the non-Abelian Berry curvatures. Due to the trigonal warping, the former also displays an anisotropic response to the orientation of the applied electric field that is qualitatively distinct from that of the latter. We further show that these anisotropic responses also reveal the essential differences between the diagonal and off-diagonal elements of the non-Abelian Berry curvature matrix in terms of their the contributions to the Hall currents. We provide a physically intuitive understanding on the origin of distinct anisotropic features from different Hall current contributions, in terms of band occupations and interband coherence. This then points to the generalization beyond the specific example of bilayer graphenes.

Introduction.—Band structure effects on transport of electrons driven by an external electric field constitute one of the most fundamental issues in solid-state physics [1]. In principle, one can group the electronic bands into two kinds of manifolds, namely, the active and the remote, according to the relation between the relevant gaps and the applied field. Due to the relatively large gaps between these two manifolds, the field-induced inter-manifold transitions are well captured by the adiabatic approximation. When the active manifold contains a single band or a number of fully degenerate bands, this adiabatic description has been successful in manifesting one of the most non-trivial band structure effects on electron transport, namely, the Hall effect [2–8], which includes a number of varieties such as spin [9–12] and valley Hall effects [13, 14]. On the other hand, when the active manifold contains a number of closely spaced but not fully degenerate bands, the effects of a finite electric field on the interband transitions within the active manifold are beyond the validity of perturbation treatment and therefore also requires non-adiabatic consideration. Correspondingly, this leads to a non-adiabatic Hall effect, which has been found to be pronounced in Dirac cones with a Berry curvature hotspot, as recently discussed [15] and extended to situations with spatially varied band structures [16].

Although previous studies have respectively expounded on the Hall effects in the adiabatic regime and expanded into the non-adiabatic one, interesting realistic materials such as transition metal dichalcogenides (ex. twisted MoSe₂ homobilayers [17–20]) and bilayer graphenes [21] indeed possess band structures that de-

mand a coherent unification of the above two perspectives. On one end, when the active manifold contains only a single band or fully degenerate bands over the whole Brillouin zone, the adiabatic inter-manifold transition results in the well-known expression of the anomalous velocity in terms of the Berry curvatures of the active bands [5, 8, 16, 22, 23]. On the other end, when the remote bands are completely ignored, non-adiabatic dynamics among the non-degenerate bands within the active manifold gives rise to a renormalized carrier velocity due to the finite electric field, that also has an anomalous part contributing to the corresponding non-adiabatic Hall effect [15]. Naturally, the consequence from the interplay of these two ends is an important question worthy further investigation, since many quantum materials of interest do have non-degenerate active bands together with non-negligible coupling to remote bands.

Apart from the non-adiabatic effects mentioned above, the multiple-band nature of the active manifold, as well-known, also gives rise to the non-Abelian characters of Berry curvatures upon projecting out the remote bands [8] (see also [16] for pedagogical derivation). On one hand, from the current response to an infinitesimal applied field, the pure geometrical aspects of the non-Abelian characters on the Hall currents have been well understood [10, 24]. On the other hand, the non-Abelian Berry curvatures as anomalous driving forces for the dynamics of single wave packets have also been analysed through the peculiarly induced motion under various contexts [25–28]. Nevertheless, the interplay between these two faces of multiple-band effects, namely, the non-Abelian characters and the non-adiabatic dynamics still

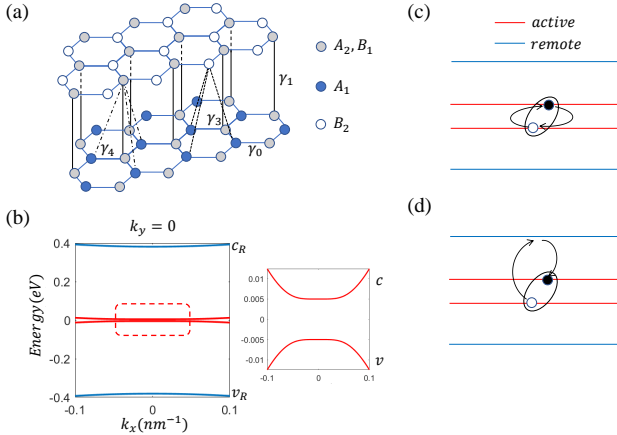


FIG. 1. (Color online) (a): The atomic structure of an AB -stacked bilayer graphene in side view. (b): The four-band dispersion (with $\gamma_3 = 0$ in (a), see also Eq. (8)) clearly distinguishing the active and the remote bands. (c): Interband coherence directly formed through non-adiabatic intra-active-manifold dynamics. (d): Interband coherence indirectly formed through adiabatic inter-manifold transitions. They imply distinct roles in their respective contributions to the Hall conduction.

remains an open question.

In this work, we address the above raised issues through investigating the valley Hall currents in biased graphene bilayer with a modest gap (0.01eV) (Fig. 1(a)) [21, 29–37]. The effective four-band model for this material features two bands close in energy forming the active manifold and two other remote bands separated from the active bands by around 0.4eV (see Fig. 1(b)), suitable for the present purpose. Furthermore, the well-known intrinsic trigonal warping of this material [21, 38] naturally exploits the experimental feasibility of studying the anisotropic current responses induced by different directions of the applied field[39, 40]. Interestingly, we found that the angular-dependence of the Hall current at finite electric fields not only reveals the crucial distinctions between the adiabatic inter-manifold and the non-adiabatic intra-active-manifold contributions to the Hall current. But it also uncovers interesting difference between contributions involving diagonals and off-diagonals from the *non-Abelian* Berry curvatures matrix.

Unified description of adiabatic and non-adiabatic regimes.— To facilitate the analysis of the Hall currents in a scenario with active and remote bands, we recall a previously developed framework that unifies the wave-packet description of electronic transport for both the adiabatic and the non-adiabatic regimes [16]. The active bands are collectively denoted by A and \mathcal{H}_A denotes the Hamiltonian of the active manifold. The dynamics of a single wave packet in the active manifold including effects from remote bands is summarised in [45]. An ensemble of wave packets gives rise to the electric currents. By taking into accounts the scattering effects and the decoherence

within the band space, the electric current driven by a finite electric field \mathbf{E} reads[16]

$$\mathbf{J} = -e \sum_i \int_{\mathbf{k}} g_i(\mathbf{k}) \bar{\mathbf{v}}_i(\mathbf{k}), \quad (1)$$

where we have abbreviated $\int d\mathbf{k}$ by $\int_{\mathbf{k}}$. Here $\bar{\mathbf{v}}_i$ is the ensemble-averaged velocity, containing two contributions, $\bar{\mathbf{v}}_i = \bar{\mathbf{v}}_i^A + \bar{\mathbf{v}}_i^R$. The intra-active-manifold non-adiabatic dynamics contributes with $\bar{\mathbf{v}}_i^A = \bar{\mathbf{v}}_i^{\text{occ},A} + \bar{\mathbf{v}}_i^{\text{coh},A}$, where

$$\bar{\mathbf{v}}_i^{\text{occ},A} = \sum_{n \in A} |\bar{\eta}_n^i|^2 \frac{\partial \varepsilon_n}{\partial \mathbf{k}}, \quad (2)$$

is the normal velocity due to band dispersion and

$$\bar{\mathbf{v}}_i^{\text{coh},A} = \sum_{n \neq m \in A} (\bar{\eta}_n^i)^* \left[\frac{\partial \mathcal{H}_A}{\partial \hbar \mathbf{k}} \right]_{n,m} \bar{\eta}_m^i, \quad (3)$$

is one part of the anomalous velocity. The other part of the anomalous velocity is contributed by the inter-manifold adiabatic dynamics with $\bar{\mathbf{v}}_i^R = \bar{\mathbf{v}}_i^{\text{occ},R} + \bar{\mathbf{v}}_i^{\text{coh},R}$, in which

$$\bar{\mathbf{v}}_i^{\text{occ},R} = \frac{e}{\hbar} \mathbf{E} \times \sum_{n \in A} |\bar{\eta}_n^i|^2 [\mathcal{F}_{\mathbf{k}}]_{n,n}, \quad (4)$$

and

$$\bar{\mathbf{v}}_i^{\text{coh},R} = \frac{e}{\hbar} \mathbf{E} \times \sum_{n \neq m \in A} (\bar{\eta}_n^i)^* [\mathcal{F}_{\mathbf{k}}]_{n,m} \bar{\eta}_m^i. \quad (5)$$

Here $\bar{\eta}_n^i$ is the complex amplitude on band n defined as the n th component of the i th eigenvector $\bar{\eta}^i$ of $\mathcal{H}_A(\mathbf{k}, \mathbf{E})$, the moving-frame Hamiltonian's projection on active bands, namely, $\mathcal{H}_A \bar{\eta}^i = \mathcal{E}_i \bar{\eta}^i$ with \mathcal{E}_i corresponding eigenvalue (see [45] for details including the explicit expressions for \mathcal{H}_A and $\mathcal{F}_{\mathbf{k}}$, the non-Abelian Berry curvature). We call $\bar{\eta}^i$'s the hybridised bands and they depend on the electric field in a non-perturbation way [15, 16, 46]. The distribution function with respect to occupations on the hybridised bands is given by $g_i = g_i^0 + \delta g_i$ where $g_i^0 = 1 / [\exp(\frac{\mathcal{E}_i - \mu}{k_B T}) + 1]$ with μ the chemical potential and T the temperature and $\delta g_i = (e/\hbar) \tau \mathbf{E} \cdot \partial g_i^0 / \partial \mathbf{k}$ with τ the relaxation time.

The current Eq. (1) can be further decomposed as $\mathbf{J} = \mathbf{J}^L + \mathbf{J}^H$, where $\mathbf{J}^L = -e \int_{\mathbf{k}} \sum_i \delta g_i \bar{\mathbf{v}}_i$ and $\mathbf{J}^H = \mathbf{J}_A^H + \mathbf{J}_R^H$, in which

$$\mathbf{J}_A^H = -e \int_{\mathbf{k}} \sum_i g_i^0 \bar{\mathbf{v}}_i^{\text{coh},A}, \quad \mathbf{J}_R^H = -e \int_{\mathbf{k}} \sum_i g_i^0 \bar{\mathbf{v}}_i^R \quad (6)$$

on knowing that $\int_{\mathbf{k}} g_i^0 \bar{\mathbf{v}}_i^{\text{occ},A} = 0$ [1]. These two contributions \mathbf{J}^L and \mathbf{J}^H respectively reproduce the well-established expressions of the longitudinal current and

the Hall current in the limit of infinitesimal \mathbf{E} [8, 16]. In this work, we are only interested in \mathbf{J}^H .

Within this framework, the issues raised in the introduction can now be addressed. The first question can be approached from the well-known notion that the Hall current is mediated by the interband coherence [7]. Both contributions \mathbf{J}_A^H and \mathbf{J}_R^H contain interband coherence among the active bands, namely, $(\bar{\eta}_n^i)^* \bar{\eta}_m^i$ for $n \neq m$ with $n, m \in A$. Such coherence in \mathbf{J}_A^H explicated by Eq. (3) is directly formed through the field-induced interband transitions within the active manifold. In contrast, for \mathbf{J}_R^H , such coherence given by Eq. (5) is only indirectly formed through transitions forth and back between the active and the remote bands (see illustrations in Fig. 1(c) and (d) respectively). This leads us to anticipate that the natures of the Hall current manifested via \mathbf{J}_A^H and \mathbf{J}_R^H can be very different.

The second question concerns the non-adiabatic dynamics and the non-Abelian characters of the Berry curvatures. This can be viewed from the decomposition $\mathbf{J}_R^H = \mathbf{J}_{\text{occ},R}^H + \mathbf{J}_{\text{coh},R}^H$, where

$$\mathbf{J}_{\text{occ/coh},R}^H = -e \int_{\mathbf{k}} \sum_i g_i^0 \bar{v}_i^{\text{occ/coh},R}. \quad (7)$$

When the active bands are fully degenerate over the Brillouin zone, $\mathbf{J}_{\text{coh},R}^H$ has no contribution to the Hall current, as we have discussed in Ref. [16]. There we have also shown that the Hall current reduces to the well-established expression $\mathbf{J}^H = (e^2/\hbar) \mathbf{E} \times \int_{\mathbf{k}} \text{Tr}(\mathcal{F}_{\mathbf{k}})$ [24] when the degenerate band energy is set below the Fermi energy. The gauge symmetry associated with band degeneracy can be utilized to study the non-Abelian characters [47]. In the following, we illustrate these points in *AB*-stacked bilayer graphenes.

The band manifolds of AB-stacked bilayer graphene.—The energy dispersion relation, including both active and remote manifolds, for *AB*-stacked bilayer graphene can be analytically obtained. In the basis of the sublattices of the two layers 1 and 2, labeled as A_1, B_1, A_2, B_2 (see Fig. 1(a)), the effective four-band Hamiltonian near the Dirac point K (or K') can be expressed as [21]

$$\mathcal{H}(\mathbf{k}) = \begin{pmatrix} \epsilon_{A_1} & f\pi^\dagger & -f_4\pi^\dagger & f_3\pi \\ f\pi & \epsilon_{B_1} & \gamma_1 & -f_4\pi^\dagger \\ -f_4\pi & \gamma_1 & \epsilon_{A_2} & f\pi^\dagger \\ f_3\pi^\dagger & -f_4\pi & f\pi & \epsilon_{B_2} \end{pmatrix} \quad (8)$$

with $\pi = \xi k_x + ik_y$, $f = \sqrt{3}a\gamma_0/2$, and $f_{3,4} = \sqrt{3}a\gamma_{3,4}/2$ in which $\xi = \pm 1$ is the valley index and a is the lattice constant. The on-site potentials can be represented explicitly as $\epsilon_{A_1} = -\frac{1}{2}U$, $\epsilon_{B_1} = \frac{1}{2}(-U + 2\Delta')$, $\epsilon_{A_2} = \frac{1}{2}(U + 2\Delta')$, and $\epsilon_{B_2} = \frac{1}{2}U$, with U the interlayer bias between the two layers and Δ' for an energy difference between dimer and non-dimer sites. The intralayer hopping between the *A* and *B* sites is given by

γ_0 and the meanings of various interlayer couplings γ_i with $i = 1, 3, 4$ are indicated in Fig. 1(a). Following Ref. [48], we fix $a = 2.46\text{\AA}$, $\gamma_0 = 3.16\text{eV}$, $\gamma_1 = 0.381\text{eV}$ and $\gamma_4 = \Delta' = 0$ throughout this work. Crucially, a nonzero γ_3 results in the trigonal warping of the energy dispersion (see Fig. 2(a)). The anisotropy of the dispersion then underlies the anisotropic response of the Hall currents as we will discuss in detail later.

The band energies obtained from diagonalising Eq. (8) is illustrated in Fig. 1(b) clearly show two bands around the Fermi energy. They are the lowest conduction band and the highest valence band, indexed by c and v respectively, that form the active manifold. The remote bands consist of the higher conduction band c_R and the lower valence band v_R (see Fig. 1(b)). The valley Hall current is $\mathbf{J}^H = \mathbf{J}_A^H + \mathbf{J}_R^H$ detailed in Eq. (6). By Eqs. (4), (5) and (6), we see \mathbf{J}_R^H is perpendicular to \mathbf{E} . As shown in an earlier study that for active manifolds with two bands, \mathbf{J}_A^H is also perpendicular to \mathbf{E} [15]. We apply the polar coordinate, i.e., $\mathbf{E} = E\hat{\rho}$ with the basis vector $\hat{\rho} = \hat{x} \cos \theta + \hat{y} \sin \theta$ and $\hat{\theta} = -\hat{x} \sin \theta + \hat{y} \cos \theta$. Here $E \equiv |\mathbf{E}|$ and θ is the angle between \mathbf{E} and \hat{x} . It is then sufficient to investigate the scalars $J_{A/R}^H = \hat{\theta} \cdot \mathbf{J}_{A/R}^H$ and $J_{\text{occ/coh},R}^H = \hat{\theta} \cdot \mathbf{J}_{\text{occ/coh},R}^H$. For definiteness, we place the chemical potential μ in the middle of the gap. Then only the lower-energy hybridised band, indexed by i_v , needs to be counted at very low temperatures in \sum_i in Eq. (6). This simplifies $J_{\text{occ/coh},R}^H = -e \int_{\mathbf{k}} \bar{v}_{i_v}^{\text{occ/coh},R}$ with $\bar{v}_{i_v}^{\text{occ/coh},R} = \hat{\theta} \cdot \bar{v}_{i_v}^{\text{occ/coh},R}$ (see Eqs. (4), (5) and (6)) and $J_A^H = -e \int_{\mathbf{k}} \bar{v}_{i_v}^{\text{coh},A}$ with $\bar{v}_{i_v}^{\text{coh},A} = \hat{\theta} \cdot \bar{v}_{i_v}^{\text{coh},A}$ (see Eqs. (3) and (6)).

Intra-versus inter-manifold contributions to the Hall currents.—Since $\mathbf{E} = E\hat{\rho}(\theta)$ is a vector, $J_{A/R}^H$ in principle depends on both E and θ . When the dispersion is isotropic ($\gamma_3 = 0$), then the dependence of J^H on θ disappears. In a previous work [15], we have studied the E -dependence of the Hall conductivity for an isotropic gapped-Dirac cone. Similar study on the E -dependence of $J_{A/R}^H$ is thus relegated here to Sec. II in [45]. Quantitatively it shows that $|J_A^H| \gg |J_R^H|$ and $|J_{\text{occ},R}^H| \gg |J_{\text{coh},R}^H|$. More importantly, when $\gamma_3 \neq 0$, then J_A^H and J_R^H should depend on θ , which characterises the orientation of the applied field, in qualitatively very different manners.

When $\gamma_3 \neq 0$ the anisotropy of the dispersion appears (see Fig. 2(a)), allowing non-trivial θ -dependence of $J_R^H = J_{\text{occ},R}^H + J_{\text{coh},R}^H$ and J_A^H . From Eqs. (5) and (7), we see on one hand, $J_{\text{occ},R}^H$ depends on θ through the band occupations $|\bar{\eta}_c^{i_v}|^2$ and $|\bar{\eta}_v^{i_v}|^2$ that have the same period in θ in $\bar{v}_{i_v}^{\text{occ},R}$. On the other hand, $J_{\text{coh},R}^H$ gains θ -dependence through the interband coherence $(\bar{\eta}_c^{i_v})^* \bar{\eta}_v^{i_v}$

in $\bar{v}_{i_v}^{\text{coh},R}$. Explicitly, we have

$$|\bar{\eta}_{c/v}^{i_v}|^2 = \frac{1 \mp \varepsilon_g/\bar{\varepsilon}_g}{2}, \quad (\bar{\eta}_c^{i_v})^* \bar{\eta}_v^{i_v} = -\frac{[\bar{\mathcal{R}}_k]_{v,c} \cdot \mathbf{E}}{\bar{\varepsilon}_g} \quad (9)$$

where $\varepsilon_g = \varepsilon_c - \varepsilon_v$ and $\bar{\varepsilon}_g = \sqrt{\varepsilon_g^2 + 4|[\bar{\mathcal{R}}_k]_{v,c} \cdot \mathbf{E}|^2}$ is the renormalized gap. Using $\mathbf{E} = E(\hat{x} \cos \theta + \hat{y} \sin \theta)$, we straightforwardly see that $(\bar{\eta}_c^{i_v})^* \bar{\eta}_v^{i_v}$ has a θ -period that is twice of that of $|\bar{\eta}_c^{i_v}|^2$ and $|\bar{\eta}_v^{i_v}|^2$. So the θ -period of J_R^H is led by that of $J_{\text{coh},R}^H$, which is associated with the interband coherence that appears in $\bar{v}_{i_v}^{\text{coh},R}$ of Eq. (5).

We now turn to the θ -dependence in J_A^H . From Eqs. (3) and (6), we find that J_A^H depends on θ through the term $(\bar{\eta}_c^{i_v})^* \bar{\eta}_v^{i_v} \hat{\theta} \cdot \partial \mathcal{H}_A / \partial \hbar \mathbf{k}$ that appears in $\bar{v}_{i_v}^{\text{coh},A}$. Here $\hat{\theta} \cdot \partial \mathcal{H}_A / \partial \hbar \mathbf{k} = (-\sin \theta \partial \mathcal{H}_A / \partial \hbar k_x + \cos \theta \partial \mathcal{H}_A / \partial \hbar k_y)$ which makes the θ -period of $(\bar{\eta}_c^{i_v})^* \bar{\eta}_v^{i_v} \hat{\theta} \cdot \partial \mathcal{H}_A / \partial \hbar \mathbf{k}$ only half as that of $(\bar{\eta}_c^{i_v})^* \bar{\eta}_v^{i_v}$. These two different θ -dependencies, are revealed correspondingly in the velocities $\bar{v}_{i_v}^{\text{coh},R}$ and $\bar{v}_{i_v}^{\text{coh},A}$, plotted as functions of θ in Fig. 2(b) and (c) respectively. It clearly shows the distinctively different periods.

The above discussed θ -period difference between $\bar{v}_{i_v}^{\text{coh},R}$ and $\bar{v}_{i_v}^{\text{coh},A}$ appears also in the difference between J_R^H and J_A^H only when the dispersion of the system is anisotropic. With $\gamma_3 \neq 0$, which leads to a well-known trigonal-warped dispersion [21, 38], we show in Fig. 3(a) at a given valley $\xi = 1$ both current contributions J_R^H and J_A^H . It clearly shows that while J_R^H follows the C_3 symmetry of the energy dispersion, J_A^H exhibits C_6 symmetry. The θ -period of the current is different from the \mathbf{k} -resolved average carrier velocity due to integration over \mathbf{k} , which manifests the symmetry of the dispersion. Nevertheless, the character that $\bar{v}_{i_v}^{\text{coh},R}$ has its θ -period twice as that of $\bar{v}_{i_v}^{\text{coh},A}$ is fully revealed in the physical observable that J_R^H 's θ -period is twice of J_A^H 's. The intuitively anticipated qualitative difference between J_A^H and J_R^H from Fig. 1(c) and (d) is thus concretely illustrated through different periods in θ .

Two faces of multiple-band effects: non-adiabatic and non-Abelian.—We now focus on the remote band contribution J_R^H to reveal the relation between the underlying non-adiabatic dynamics and the non-Abelian characters raised from the multi-band effects in the active manifold. As we have mentioned before, when the active bands are fully degenerate and occupied, the linear conductivity is given by $\sigma^H = \partial J^H / \partial E|_{E=0} = (e^2/\hbar) \int_{\mathbf{k}} \text{Tr}(\mathcal{F}_{\mathbf{k}}^z)$, which depends neither on E nor on θ , as a consequence of its definition. Furthermore, this linear conductivity only involves the band diagonals of the Berry curvature matrix $\mathcal{F}_{\mathbf{k}}^z$.

As discussed before, anisotropy of the dispersion can be revealed in the Hall currents under the finite electric fields. In order to extract the θ -dependence more exclu-

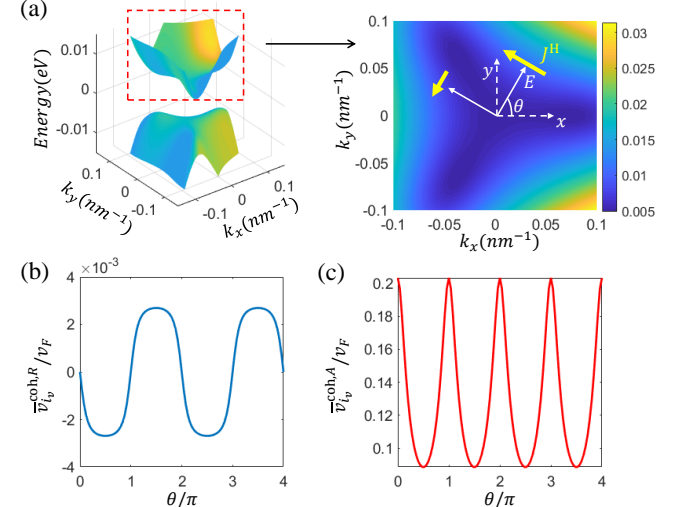


FIG. 2. (Color online) (a): The anisotropic dispersion of the bands near the fermi energy, demonstrated with $\gamma_3 = 0.38\text{eV}$ [48]. Inset: The trigonal warping of active conduction band, implying that the magnitude of the Hall current (yellow arrows of different lengths) depends on the angle θ between \mathbf{E} (solid white arrows) and the crystal axis, here taken as \hat{x} (dashed white arrow). (b) and (c): Different θ -dependencies of the anomalous velocities $\bar{v}_{i_v}^{\text{coh},R}$ and $\bar{v}_{i_v}^{\text{coh},A}$ respectively, giving rise to distinct periods in θ and determining the anisotropic responses of J_R^H and J_A^H to θ (see the main text for details). The specific choice of \mathbf{k} is irrelevant. Here we use $k_x = 0.01\text{\AA}$ and $k_y = 0$. The energy gap is $U = 0.01\text{eV}$. The field-strength is $E = 1.15\text{V}/\mu\text{m}$ here [45] and $v_F = \sqrt{3}a\gamma_0/\hbar$ as the Fermi velocity.

sively, we define $\Delta J_{\text{coh/occ},R}^H = J_{\text{coh/occ},R}^H - \bar{J}_{\text{coh/occ},R}^H$, where we subtract the angular average $\bar{J}_{\text{coh/occ},R}^H = (1/\theta_T^{\text{coh/occ},R}) \int_0^{\theta_T^{\text{coh/occ},R}} d\theta J_{\text{coh/occ},R}^H$ in which $\theta_T^{\text{coh/occ},R}$ denotes the θ -period of $J_{\text{coh/occ},R}^H$. We plot $\Delta J_{\text{coh},R}^H$ (solid line) and $\Delta J_{\text{occ},R}^H$ (dashed line) as a function of θ in Fig. 3(b), which shows that $\theta_T^{\text{coh},R} = 2\theta_T^{\text{occ},R}$, as expected due to the reasons already discussed for Fig. 2. More interestingly, in Fig. 3(b) we see that $\Delta J_{\text{coh},R}^H$ displays a variation with respect to θ that is clearly greater than that of $\Delta J_{\text{occ},R}^H$. This is because the interband coherence $(\bar{\eta}_c^{i_v})^* \bar{\eta}_v^{i_v}$ in general is more sensitive to θ than the occupation $|\bar{\eta}_{c/v}^{i_v}|^2$ since the former is one order larger in $E \cos \theta$ and $E \sin \theta$ than the latter (see Eq. (9)). The underlying non-adiabatic dynamics, characterised by θ -dependence at finite \mathbf{E} , thus manifests the non-Abelian characters of $\mathcal{F}_{\mathbf{k}}^z$, differentiating between the diagonal $J_{\text{occ},R}^H$ and off-diagonal $J_{\text{coh},R}^H$ contributions.

Conclusions and discussions.—In summary, through the studies of the valley Hall currents in typical AB -stacked bilayer graphenes as an example, we have demonstrated the followings. (i): J_R^A and J_R^H not only differ quantitatively about an order of magnitude, they also differ qualitatively in terms of the periodicity with re-

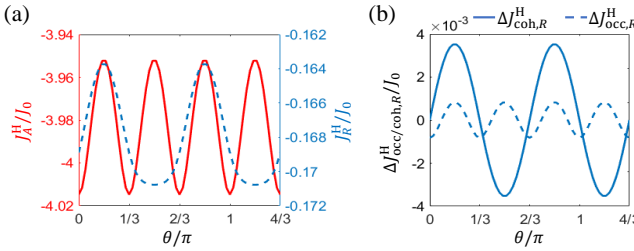


FIG. 3. (Color online) (a): The qualitative difference between J_R^H and J_A^H revealed through distinct symmetries (C_3 for J_R^H and C_6 for J_A^H). (b): Angular variations of inter-band coherence ($\Delta J_{coh,R}^H$ as the solid line) and band-occupation ($\Delta J_{occ,R}^H$ as the dashed line) contributions, respectively to the remote-band-mediated Hall current J_R^H , contrasting the diagonal and the off-diagonal involvements of the non-Abelian Berry curvature matrices. The parameters are same as what we take in Fig. 2 for both (b) and (c). The angular averages are $\bar{J}_{occ,R}^H = 0.168J_0$ and $\bar{J}_{coh,R}^H = 0$.

spect to the angle of the applied electric field. (ii): The non-Abelian characters are manifested by the difference between $J_{occ,R}^H$ and $J_{coh,R}^H$ in terms not only of the periodicity with respect to the angle of the applied electric field but also of the angular variation amplitude.

The values of the angular periods and the shapes of the angular profiles for different contributions to the Hall currents depend on the details of the materials' electronic structures under consideration. Nevertheless, the conclusions (i) and (ii), confirmed by the calculations specifically designated to AB -stacked bilayer graphenes, are expected to be held also for other materials with anisotropic energy dispersion such that the Hall current at finite electric fields is sensitive to the orientation of the field. This is because the general analysis leading to the above conclusions is simply rooted to how band occupation and interband coherence differ fundamentally in their responses to the applied electric field (as exemplified for two-band active manifold in Eq. (9)). This fundamental difference also serves as the basis to manifest the multiple-band induced non-Abelian effects in Hall currents. Interestingly, this provides an intuitive approach toward the understanding of the non-Abelian characters, totally based on physically observable carrier transport currents, as complementary to the conventional understanding based on quantum geometry of the band structures.

Acknowledgments.—C. Li would like to thank D. W. Zhai and B. Fu for useful discussions. The work is mainly supported by the Research Grants Council of Hong Kong (HKU17306819 and AoE/P-701/20), and the University of Hong Kong (Seed Funding for Strategic Interdisciplinary Research). M. W.-Y. Tu acknowledge the the hospitality of Prof. Tay-Rong Chang with support from ministry of technology and science in Tai-wan of grand no. MOST110-2636-M-006-016. M. W.-Y. Tu also acknowledge the hospitality of National Center for Theoretical Science and thank Prof. Tse-Min Chen for useful

discussions.

* oldsmith@hku.hk

† kerustemiro@gmail.com

- [1] N. W. Ashcroft and N. D. Mermin, *Solid State Physics* (Sounders College, Philadelphia, 1976).
- [2] R. Karplus and J. M. Luttinger, Hall effect in ferromagnetics, *Phys. Rev.* **95**, 1154 (1954).
- [3] J. M. Luttinger, Theory of the Hall effect in ferromagnetic substances, *Phys. Rev.* **112**, 739 (1958).
- [4] E. Adams and E. Blount, Energy bands in the presence of an external force field-II: Anomalous velocities, *J. Phys. Chem. Solids* **10**, 286 (1959).
- [5] D. J. Thouless, M. Kohmoto, M. P. Nightingale, and M. D. Nijs, Quantized Hall Conductance in a Two-Dimensional Periodic Potential, *Phys. Rev. Lett.* **49**, 405 (1982).
- [6] T. Jungwirth, Q. Niu, and A. H. MacDonald, Anomalous Hall Effect in Ferromagnetic Semiconductors, *Phys. Rev. Lett.* **88**, 207208 (2002).
- [7] N. Nagaosa, J. Sinova, S. Onoda, A. H. MacDonald, and N. P. Ong, Anomalous Hall effect, *Rev. Mod. Phys.* **82**, 1539 (2010).
- [8] D. Xiao, M.-C. Chang, and Q. Niu, Berry phase effects on electronic properties, *Rev. Mod. Phys.* **82**, 1959 (2010).
- [9] S. Murakami, N. Nagaosa, and S.-C. Zhang, Dissipationless quantum spin current at room temperature, *Science* **301**, 1348 (2003).
- [10] S. Murakami, N. Nagaosa, and S. C. Zhang, *Phys. Rev. B* **69**, 235206 (2004).
- [11] J. Sinova, D. Culcer, Q. Niu, N. A. Sinitsyn, T. Jungwirth, and A. H. MacDonald, Universal Intrinsic Spin Hall Effect, *Phys. Rev. Lett.* **92**, 126603 (2004).
- [12] C. L. Kane and E. J. Mele, Z_2 Topological Order and the Quantum Spin Hall Effect, *Phys. Rev. Lett.* **95**, 146802 (2005).
- [13] D. Xiao, W. Yao, and Q. Niu, Valley-Contrasting Physics in Graphene: Magnetic Moment and Topological Transport, *Phys. Rev. Lett.* **99**, 236809 (2007).
- [14] D. Xiao, G.-B. Liu, W. Feng, X. Xu, and W. Yao, Coupled Spin and Valley Physics in Monolayers of MoS₂ and Other Group-VI Dichalcogenides, *Phys. Rev. Lett.* **108**, 196802 (2012).
- [15] M. W. Y. Tu, C. Li, H. Y. Yu, and W. Yao, Non-adiabatic Hall effect at Berry curvature hot spot, *2D Materials* **7**, 4 (2020).
- [16] M. W. Y. Tu, C. Li, and W. Yao, Theory of wavepacket transport under narrow gaps and spatial textures: Nonadiabaticity and semiclassicality, *Phys. Rev. B* **102**, 045423 (2020).
- [17] Y. Wang, Z. Wang, W. Yao, G. B. Liu, and H. Y. Yu, Interlayer coupling in commensurate and incommensurate bilayer structures of transition-metal dichalcogenides, *Phys. Rev. B* **95**, 115429 (2017).
- [18] F. C. Wu, T. Lovorn, E. Tutuc, I. Martin, and A. H. MacDonald, Topological Insulators in Twisted Transition Metal Dichalcogenide Homobilayers, *Phys. Rev. Lett.* **122**, 086402 (2019).
- [19] D. W. Zhai and W. Yao, Theory of tunable flux lattices in the homobilayer moiré of twisted and uniformly

- strained transition metal dichalcogenides, *Phys. Rev. Mat* **4**, 094002 (2020).
- [20] H. Y. Yu, M. X. Chen, and W. Yao, Giant magnetic field from moiré induced Berry phase in homobilayer semiconductors, *Natl. Sci. Rev* **7**, 12-20 (2020).
- [21] E. McCann and M. Koshino, The electronic properties of bilayer graphene, *Rep. Prog. Phys.* **76**, 5 (2013).
- [22] Q. Niu, M. C. Cheng, B. Wu, D. Xiao, and R. Cheng, *Physical Effects of Geometric Phases* (World Scientific, 2017).
- [23] A. Böhm, H. Koizumi, Q. Niu, J. Zwanziger, and A. Mostafazadeh, *The Geometric Phase in Quantum Systems* (Springer, 2003).
- [24] R. Shindou and K. I. Imura, Noncommutative geometry and non-Abelian Berry phase in the wave-packet dynamics of Bloch electrons, *Nucl. Phys. B* **720**, 399 (2005).
- [25] D. Culcer, Y. Yao, and Q. Niu, Coherent wave-packet evolution in coupled bands, *Phys. Rev. B*, **72**, 085110 (2005).
- [26] M.-C. Chang and Q. Niu, Berry curvature, orbital moment, and effective quantum theory of electrons in electromagnetic fields, *J. Phys.: Condens. Matter* **20**, 193202 (2008).
- [27] E. V. Gorbar, V. A. Miransky, I. A. Shovkovy, and P. O. Sukhachov, Non-Abelian properties of electron wave packets in the Dirac semimetals A_3Bi ($A=Na, K, Rb$), *Phys. Rev. B* **98**, 045203 (2018).
- [28] T. Stedman, C. Timm and L. M. Woods, Multiband effects in equations of motion of observables beyond the semiclassical approach, *New J. Phys.* **21**, 103007 (2019).
- [29] K. S. Novoselov, et. al, Unconventional quantum Hall effect and Berry's phase of 2π in bilayer graphene, *Nat. Phys.* **2**, 177 (2006).
- [30] E. McCann and V. I. Fal'ko, Landau-Level Degeneracy and Quantum Hall Effect in a Graphite Bilayer, *Phys. Rev. Lett.* **96**, 086805 (2006).
- [31] T. Ohta, A. Bostwick, T. Seyller, K. Horn, and E. Rotenberg, Controlling the Electronic Structure of Bilayer Graphene, *Science* **313**, 951 (2006).
- [32] E. McCann, Asymmetry gap in the electronic band structure of bilayer graphene, *Phys. Rev. B* **74**, 161403(R) (2006).
- [33] E. V. Castro, et al, Biased Bilayer Graphene: Semiconductor with a Gap Tunable by the Electric Field Effect, *Phys. Rev. Lett.* **99**, 216802 (2007).
- [34] J. B. Oostinga, H. B. Heersche, X. L. Liu, A. F. Morpurgo, and L. M. K. Vandersypen, Gate-induced insulating state in bilayer graphene devices, *Nat. Mater.* **7**, 151 (2008).
- [35] Y. B. Zhang, et al, Direct observation of a widely tunable bandgap in bilayer graphene, *Nature* **459**, 820 (2009).
- [36] L. Yang, J. Deslippe, C. H. Park, M. L. Cohen, and S. G. Louie, Excitonic Effects on the Optical Response of Graphene and Bilayer Graphene, *Phys. Rev. Lett.* **103**, 186802 (2009).
- [37] L. Ju, et al, Topological valley transport at bilayer graphene domain walls, *Nature* **520**, 650 (2015).
- [38] K. Kechedzhi, V. I. Fal'ko, E. McCann, and B. L. Altshuler, Influence of Trigonal Warping on Interference Effects in Bilayer Graphene, *Phys. Rev. Lett.* **98**, 176806 (2007).
- [39] K. Kang, T. Li, E. Sohn, J. Shan, and K. F. Mak, Nonlinear anomalous Hall effect in few-layer WTe₂, *Nat. Mater.* **18**, 324 (2019).
- [40] The experiment [39] targets at the study of the well-known nonlinear Hall effect [41–43] supported by *Abelian* Berry curvature dipoles, which aims at the higher-order action of an ac electric field on the off-equilibrium distribution where extrinsic scattering plays important roles. It keeps a single band in the active manifold so the remote band effects are well accounted adiabatically, giving rise to the *Abelian* Berry curvature [43, 44]. Here instead we are interested in the non-perturbation action of a dc electric field on intrinsic inter-band transitions within the multiple-band active manifold, where remote band effects are manifested by *non-Abelian* Berry curvatures.
- [41] E. Deyo, L. E. Golub, E. L. Ivchenko, and B. Spivak, Semiclassical theory of the photogalvanic effect in non-centrosymmetric systems, arXiv:0904.1917v1 (2009).
- [42] J. E. Moore and J. Orenstein, Confinement-induced Berry phase and helicity-dependent photocurrents, *Phys. Rev. Lett.* **105**, 026805 (2010).
- [43] I. Sodemann and L. Fu, Quantum Nonlinear Hall Effect Induced by Berry Curvature Dipole in Time-Reversal Invariant Materials, *Phys. Rev. Lett.* **115**, 216806 (2015).
- [44] Z. Z. Du, C. M. Wang, S. Li, H.-Z. Lu, and X. C. Xie, Disorder-induced nonlinear Hall effect with time-reversal symmetry, *Nat. Commun.* **10**, 3047 (2019).
- [45] The Supplementary contains the followings. (i): Summary of a previously developed framework in Ref. [15, 16], allowing non-adiabatic description of wave packet dynamics and currents from ensemble of wave packets. (ii): Studies of the dependence of the Hall current components on E , the strength of the electric field \mathbf{E} . (iii): Agreement between the computation of the Hall currents obtained with and without separating the bands into active and remote manifolds. This verifies that it is meaningful to categorise the bands in the way we have described.
- [46] The physical meaning of $\bar{\eta}^i$ can be seen as following. The joint action of decoherence and the electric field favours a certain form of interband coherence as those contained in $\bar{\eta}^i$'s. As a result, the carriers are led to a statistical mixture of the hybridised bands $\bar{\eta}^i$'s.
- [47] F. Wilczek and A. Zee, Appearance of gauge structure in simple dynamical systems, *Phys. Rev. Lett.* **52**, 2111 (1984).
- [48] A. B. Kuzmenko, I. Crassee, D. van der Marel, P. Blake, and K. S. Novoselov, Determination of the gate-tunable band gap and tight-binding parameters in bilayer graphene using infrared spectroscopy, *Phys. Rev. B* **80**, 165406 (2009).